Evidence of Simultaneous Double-Electron Promotion in F^+ Collisions with Surfaces

J. Mace, M. J. Gordon, and K. P. Giapis*

Division of Chemistry and Chemical Engineering, California Institute of Technology, Pasadena, California 91125, USA

(Received 15 August 2006; published 22 December 2006)

A high-flux beam of mass-filtered F^+ at low energy (100–1300 eV) was scattered off Al and Si surfaces to study core-level excitations of F^0 and F^+. Elastic scattering behavior for F^+ was observed at energies <300 (500) eV off Al (Si) for a 90° lab angle. However, above this energy threshold, orbital mixing in the hard collision step results in electronic excitation of F via molecular orbital promotion along the $4f\sigma$ (F-$2p$), significantly reducing the observed ion exit energy. In addition, despite the electronegativity of F, scattering at energies >450 (700) eV off Al (Si) produces F^{2+}—behavior which is remarkably similar to Ne^+ off the same surfaces. Inelasticities measured for single collision events agree well with the energy deficits required to form (doubly excited) F^{**} and F^{+**} states from F^0 and F^+, respectively; these excited species most likely decay to inelastic F^+ and F^{2+} via autoionization.

DOI: 10.1103/PhysRevLett.97.257603 PACS numbers: 79.20.Rf, 34.50.Dy, 34.50.Fa, 34.70.+e

Scattering of electronegative gas atoms and ions (i.e., O, F, Cl) off surfaces is generally accompanied by highly efficient electron capture processes; as such, the scattered particle flux is largely composed of anions and neutrals [1–6]. Negative ion formation via resonant capture is quite probable because image charge effects near a metal surface tend to shift the projectile anion level below the Fermi level of the surface [6]. As such, charge exchange in these systems is largely governed by nonlocal processes as the projectile approaches or rebounds from the surface. However, local interactions involving double-electron promotion have been shown to be important in some systems, resulting in significant positive ion production. For instance, Ne^+ scattering off light targets (Mg, Al, Si, and P) at low energy results in very high positive ion yields (Ne^+ and even Ne^{2+}) [7,8]. Since the electron energy level ordering of F and Ne is identical with respect to these targets, electron promotions in F should also occur. In fact, such effects should be seen at collision energies even lower than those for Ne^+.

In this Letter, we show that double promotion along the $4f\sigma$ molecular orbital (MO) does occur for both F^0 and F^+ when F^+ is scattered off Al and Si surfaces. Inelastic F^+ and F^{2+} exit channels were observed at low collision energies (>450–700 eV/90° lab angle); energy losses for single-scatter events show that $F^0 \rightarrow F^{**}$ and $F^+ \rightarrow F^{+**}$, followed by autoionization, are responsible for the 1+ and 2+ exits, respectively. Furthermore, the threshold R_{min} calculated for $4f\sigma$ MO promotion in the F-Si quasimolecule agree quite well with the experimental onset of F^{2+} production ($R_{min} = 0.5$–0.6 Å).

Experiments were performed in a custombuilt ion beam-line scattering apparatus described in detail elsewhere [9]. Ions were produced in a 13.56 MHz rf-driven inductively coupled plasma discharge with a feed of 1:1 CF_4:O_2 (5 sccm), operating at 2 mTorr and 600 W. Ion energy was adjusted by floating the plasma above ground with dc. After ion extraction, magnetic mass-filtering, and fast neutral removal, a 2–3 μA beam of F^+ (3 mm diameter) was delivered at 45° onto a grounded target (n-type Si wafer or polycrystalline Al, freshly sputtered and annealed). Scattered products were monitored at a 90° lab angle with a triply differentially pumped 90° hemispherical-sector energy analyzer in series with a quadrupole mass spectrometer.

Figure 1 shows the mean exit energies of F^+ and F^{2+} resulting from single-scatter (SS) collisions of F^+ projectiles ($E_0 = 100$–1300 eV) with Si, along with the elastic prediction for $\theta_{lab} = 90°$ (kinematic factor $K = 0.191$ [10]). Two distinct regions with respect to incident energy are readily apparent where the collision kinematics are quite different. For $E_0 < 500$ eV, scattering is essentially elastic with minor losses attributable (at first glance) to

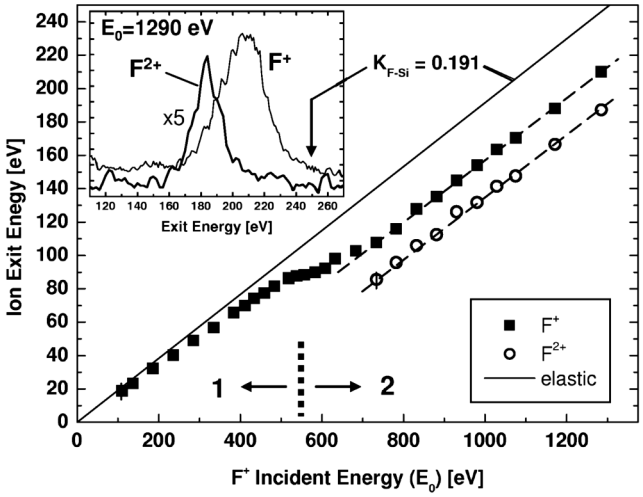

FIG. 1. Exit energies of F^+ and F^{2+} resulting from single binary collisions of F^+ projectiles with Si at a 90° lab angle along with elastic prediction (solid line). Error bars are partially shown to avoid clutter. (Inset) Exit energy distributions for F^+/F^{2+} when $E_0 = 1290$ eV.

electron straggling (electron drag) [11] on the incoming and outgoing trajectory paths as the projectile encounters the target bands. However, careful inspection of the energy offset in region 1 reveals that straggling losses (a few eV in our case [8]) cannot be solely responsible for the deviation. Identical experiments with Ne^+ projectiles on bare and fluorinated Si (F/Si) show that the surface Si_xF_y layer (which commonly forms in F etching environments [12]) significantly increases straggling: i.e., Ne^+ off bare Si is perfectly elastic (within 3–5 eV [9]), while Ne^+ and F^+ off F/Si show much larger deviations. This observation can be rationalized on the grounds that chemisorbed fluorine will draw a considerable amount of electron density toward the surface which could likely increase the total electron drag on the projectile. In any case, we see that region 1 is effectively elastic in nature overall because the collision apsis (distance of closest approach $R_{\min}$) is relatively large at low E_0 (i.e., $R_{\min} \sim 0.65$ Å@400 eV/90°, Thomas-Fermi-Molière potential with Firsov screening length [10]); as such, significant overlap of the core-shell atomic orbitals (AO's) of the collision partners (F + Si) has not yet occurred.

However, when the collision energy is raised above a critical value ($E_0 \sim 700$ eV), the overall kinematics of the system change entirely—F^+ becomes quite inelastic and F^{2+} suddenly appears with an even greater energy offset. The measured average exit energy of F^+ is 35–40 eV lower than that predicted by the binary collision approximation (BCA) for a 90° elastic deflection [9]. The simultaneous appearance of these two phenomena above a critical collision energy is a clear indicator of electronic transitions taking place in the hard collision step as the AO's of the colliding partners intermix at small $R_{\min}$. For instance, AO overlap at a close distance (<0.5 Å) gives rise to hybrid MO's during the close encounter portion of the scattering trajectory when a short-lived ($\sim 10^{-15}$ s) quasimolecule is formed. In certain cases, particular MO's of the quasimolecule may be highly promoted in energy (due to degeneracy) so as to cross other MO's which will ultimately decay into Rydberg states as the atoms separate (Barat-Fano-Lichten theory [13]). At these crossings, electron exchange can occur, leaving one of the exiting species in an excited state after the collision with a kinetic energy deficit. Indeed, very similar behavior has been seen for Ne^+ off Mg, Al, Si, and P targets [8]. In this situation, inelastic Ne^+/Ne^{2+} below a critical apsis is caused by double promotion of electrons from the Ne $2p_z$ ($4f\sigma$ MO) to the Ne $3s$ in the hard collision step (i.e., $2p^6 \rightarrow 2p^4 3s^2$ and $2p^5 \rightarrow 2p^3 3s^2$). These excited states (Ne^{**} and Ne^{+**}) then decay far from the surface via autoionization to give Ne^+ and Ne^{2+} with large kinetic energy deficits that directly correlate with the energy requirements for excitation [$Ne^0 \rightarrow Ne^{**}$ (41–45 eV) and $Ne^+ \rightarrow Ne^{+**}$ (69–72 eV)]. The fact that both the F^+ and F^{2+} energy losses remain relatively constant with E_0, so long as the threshold $R_{\min} \sim 0.52$ Å (700 eV at 90°) has been reached, further suggests that well-defined electronic excitations are at play in the F + Si system.

Additional evidence for a fundamental excitation mechanism comes from energy loss measurements using an Al target. Since the energy ordering of AO's of Al and Si is identical with respect to the F projectile (i.e., the MO correlation diagram is the same [13]), collision kinematics for SS events off Al and Si should be quite similar. Indeed, this is the case (Fig. 2), except that the F^+ inelasticity and F^{2+} production begin at a lower collision energy (larger $R_{\min} \sim 0.59$–0.62 Å). This latter effect is simply due to the L shell of Si being closer to the nucleus than that for Al. Small differences also occur at low E_0; F^+ scattering off Al is almost perfectly elastic. It is likely that the fluorinated layer (Al_xF_y) on the Al surface is significantly thinner than that for Si because F spontaneously reacts with Si [12] but not with Al. Smaller straggling losses would be expected due to lower electron density in the surface region because of less F on the surface. We also see that the scattered F^+ intensity [14] makes a large jump when inelastic losses become significant (Si is analogous). In general, the scattered ion yield increases exponentially with inverse projectile velocity because of contact time arguments [10]; i.e., a slower projectile has a larger probability of being neutralized by Auger or resonant charge transfer with the surface as a whole. However, the rapid increase in F^+ at the threshold indicates the sudden turn-on of "additional" F^+ generation. Finally, it should be noted that the total F^{2+} production continually increases with collision energy and that it is smaller (~10–50x less) than F^+.

Previous experimental studies of F collision kinematics at low energy are sparse [1,15] and F^{2+} off Si has been reported only once [16]. Hird *et al.* detected F^{2+} off Si using F^+ projectiles when $R_{\min} < 0.25$ Å ($E_0 > 3.8$ keV at $\theta_{\text{lab}} = 63°$); as a comparison, the same study found that Ne^{2+} was formed when $R_{\min} < 0.573$ Å ($E_0 > 800$ eV at $\theta_{\text{lab}} = 48°$). This large apsis discrepancy between F and

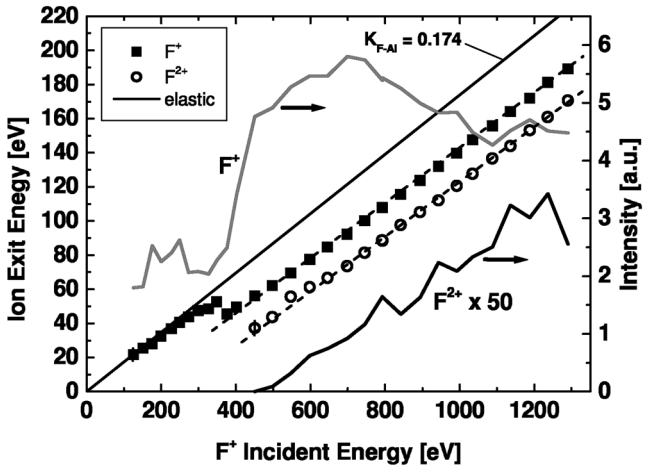

FIG. 2. Exit energies and intensities of F^+ and F^{2+} resulting from single binary collisions of F^+ with Al at a 90° lab angle.

Ne is contrary to intuition given that the energy ordering of AO's for F and Ne with respect to Si is identical. In our experiments, the onset of inelastic F^+ and F^{2+} generation occurs at much larger apsides—on par with those expected in light of Ne^+/Ne^{2+}. To look more carefully at possible mechanisms for F^+/F^{2+}, raw energy losses measured in the lab reference frame must be converted to the center-of-mass system and adjusted for straggling. When $\theta_{lab} = 90°$, the binary collision inelasticity (Q_{bin}), i.e., the total energy that is directly available for electronic excitation in the hard collision, can be evaluated quite simply [10]:

$$E_{exit} = K(E_0 - Q_1) - \frac{\gamma}{\gamma + 1} Q_{bin} - Q_3, \qquad (1)$$

where E_0 is the projectile energy, $K = (\gamma - 1)/(\gamma + 1)$ is the kinematic factor, $\gamma = M_t/M_p$ is the target-to-projectile mass ratio, and $Q_{1,3}$ represents the straggling losses [17] on the incoming (1) and outgoing (3) parts of the collision trajectory. Inelasticity values determined in this fashion are given in Fig. 3 along with the energy requirements for several $F^0/F^-/F^+$ excitation channels [18] using the Ne^0/Ne^+ system for inspiration. Transition energies have been referenced to the slowly increasing baseline because of the aforementioned augmented straggling affects due to surface fluorination. On this graph, one immediately sees that the Q_{bin} values for F^+ and F^{2+} are large, relatively constant, and fall within well-defined ranges when $R_{min} < 0.55$ Å. Incidentally, this apsis value is exactly that predicted for L-L shell overlap of F + Si (crosshatched region) [19], suggesting that AO mixing is ultimately responsible for the opening of new excitation channels.

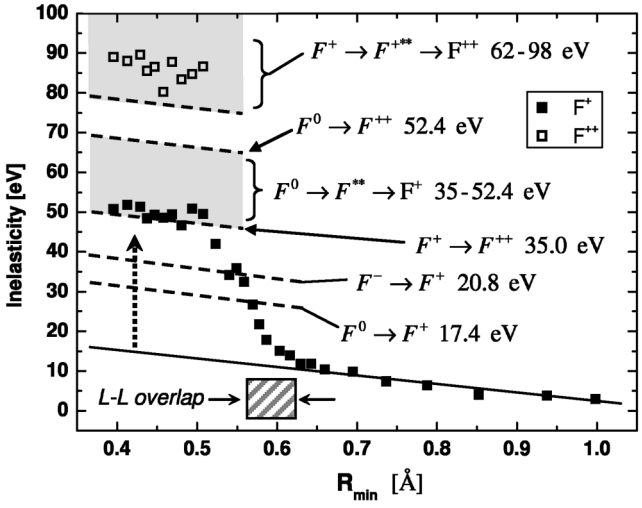

FIG. 3. Binary inelasticities (Q_{bin}) of F^+ and F^{2+} off Si determined with Eq. (1). Transition energies for several projectile excitations are shown. Grey areas represent the range of Q_{bin} values possible due to the presence of several different doubly excited final states. The crosshatched region denotes the collision apsides where the maximum electron density overlap of the F ($2s/2p$) and Si ($2s/2p$) orbitals would occur.

As indicated, the energy loss data can be conveniently assigned to transitions initiating from ground state F^0 or F^+ (subject to the sloping baseline):

$$F^+ \xrightarrow{neut} F^0 \xrightarrow{MO} F^{**}(2p^3 3s^2) \xrightarrow{AI} F^+, \qquad Q_{bin} \geq 35 \text{ eV},$$

$$F^+ \xrightarrow{MO} F^{+**}(2p^2 3s^2) \xrightarrow{AI} F^{2+}, \qquad Q_{bin} \geq 62 \text{ eV}.$$

In the first case, F^+ is neutralized to F^0 on approach to the surface through nonlocal processes (Auger and/or resonant charge transfer [10]), followed by double excitation to F^{**} via molecular orbital promotion (analogous to $Ne^0 \rightarrow Ne^{**}$) in the hard collision step. Since the lifetime of F^{**} is likely to be longer than the collision time (i.e., the Ne^{**} lifetime is $>10^{-14}$ s [20], so F^{**} should be similar), F^{**} can leave the surface intact and subsequently autoionize (AI) to F^+ far from the surface. This mechanism is probable because most projectile ions approaching the surface will be efficiently neutralized before the hard collision occurs [10]. For F^{2+}, an analogous process occurs where the precursor state entering the hard collision is instead F^+, which has survived neutralization on the incoming trajectory path. This hypothesis is strongly supported by the much smaller F^{2+} signal intensity compared to F^+ (inset in Fig. 1). Although double collisions are frequently suggested as the cause of a 2+ channel [21] (i.e., F^0 goes to F^+ in the first collision, followed by F^+ to F^{2+} by direct ionization in the second), we see that the magnitude of the 2+ energy loss is too great for such an explanation [62–98 eV vs. 17.4 (collision no. 1) + 35 (no. 2) = 52.4 eV]. In fact, these two mechanisms are identical to those proposed for Ne^+ inelasticity and Ne^{2+} formation off Si; indeed, one

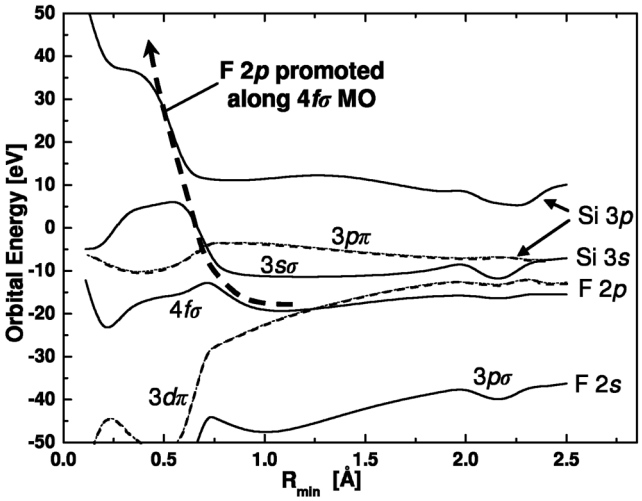

FIG. 4. Orbital energies for the F-Si molecule as a function of internuclear distance. The calculated σ orbitals (π orbitals) are indicated by solid (dashed) lines; the atomic character of each MO is shown to the right. Strong promotion (heavy dashed line) along the $4f\sigma$ MO occurs near $R_{min} \sim 0.6$ Å, allowing projectile excitation to the F^{**} ($2p^3 3s^2$) and F^{+**} ($2p^2 3s^2$) states.

would surmise that such processes should be rather generic when orbital energy orderings and promotion are similar. To further support this claim, molecular orbital calculations [22] were carried out to determine the range of $R_{\min}$ needed for $4f\sigma$ MO promotion (Fig. 4). These results demonstrate that excitation of the F $2p$ along the $4f\sigma$ MO should occur for $R_{\min} = 0.5$–0.6 Å—identical to the experiment.

Given the above mechanism, it is now possible to explain the F^+/F^{2+} intensity variations with collision energy (Fig. 2). The sudden increase in scattered F^+ can be associated with opening of the $F^0 \rightarrow F^{**} \rightarrow F^+$ channel. For F^{2+}, the continual increase with E_0 results from less efficient neutralization of the projectile F^+ as the energy is raised. The large difference overall between the F^+ and F^{2+} intensities is due to the F^+ projectile being neutralized to F^0 most of the time—and F^0 cannot produce F^{2+} in a single collision event. Finally, the tapering off of the F^+ signal at high energies is similar to the case of Ne^+ off Si, which has been explained as due to collision-induced neutralization in the hard collision step [8], i.e., resonant transfer from the target bands to the $4f\sigma$ MO (filling the F $2p_z$)—which can occur only if the $4f\sigma$ is highly promoted at small $R_{\min}$. Although the present study has emphasized only ions and their associated energy losses, identical processes surely occur for neutral projectiles with respect to an inelastic F^+ exit, i.e., formation of F^{**} (which autoionizes to F^+) that descends from an F^0 precursor. Therefore, energetic neutrals formed by ion neutralization will show similar interaction dynamics and inelastic losses.

In conclusion, scattering of F ions off Si and Al surfaces at low energies follows the BCA closely until a threshold is reached where electron promotions result in significant inelasticity for the exiting projectile. Core-level electronic excitations of F^0 and F^+ via double promotion were seen to be responsible for the inelastic F^+ and F^{2+} exit channels, respectively, when $R_{\min} < 0.52$ Å (700 eV/90°) and 0.60 Å (450 eV/90°) for the F-Si and F-Al collision pairs, respectively. Despite its electronegativity, F^+ scattering off Al and Si is qualitatively identical to Ne^+ from the perspective of a well-defined 2+ turn-on, continually increasing 2+ yield with impact energy, and inelasticity values which point to the same $4f\sigma$ double promotion mechanism. Thus, in the range of energies where electron promotion is observed, it appears that chemical interactions are irrelevant. Finally, for incident energies larger than threshold, scattered F atoms and ions will possess kinetic energies lower than those predicted by BCA. Since scattered ions are important in patterning of semiconductor devices using plasma etching, energy losses suffered in sidewall collisions will influence the etch rate and pattern profile [23].

This work was based on research funded by the National Science Foundation (No. CTS-0317397).

*Corresponding author.
Electronic address: giapis@cheme.caltech.edu

[1] M. Maazouz, S. Ustaze, L. Guillemot, and V. A. Esaulov, Surf. Sci. **409**, 189 (1998).
[2] C. Auth, A. G. Borisov, and H. Winter, Phys. Rev. Lett. **75**, 2292 (1995).
[3] P. Roncin, A. G. Borisov, H. Khemliche, A. Momeni, A. Mertens, and H. Winter, Phys. Rev. Lett. **89**, 043201 (2002).
[4] A. G. Borisov, V. Sidis, P. Roncin, A. Momeni, H. Khemliche, A. Mertens, and H. Winter, Phys. Rev. B **67**, 115403 (2003).
[5] H. Winter, A. Mertens, C. Auth, and A. G. Borisov, Phys. Rev. A **54**, 2486 (1996).
[6] S. Ustaze, R. Verucchi, S. Lacombe, L. Guillemot, and V. A. Esaulov, Phys. Rev. Lett. **79**, 3526 (1997).
[7] L. Guillemot, S. Lacombe, V. A. Esaulov, and I. F. Urazgildin, Surf. Sci. **334**, 224 (1995).
[8] M. J. Gordon, J. Mace, and K. P. Giapis, Phys. Rev. A **72**, 012904 (2005), and references therein.
[9] M. J. Gordon and K. P. Giapis, Rev. Sci. Instrum. **76**, 083302 (2005).
[10] J. W. Rabalais, *Principles and Applications of Ion Scattering Spectrometry: Surface Chemical and Structural Analysis* (Wiley, New York, 2003).
[11] O. Oen and M. Robinsen, Nucl. Instrum. Methods **132**, 647 (1976).
[12] F. R. McFeely, J. F. Morar, N. D. Shinn, G. Landgren, and F. J. Himpsel, Phys. Rev. B **30**, 764 (1984).
[13] M. Barat and W. Lichten, Phys. Rev. A **6**, 211 (1972).
[14] Scattered intensities were corrected by the cross section and normalized for beam current. See Ref. [8].
[15] J. P. Grouard, V. A. Esaulov, R. I. Hall, J. L. Montmagnon, and V. N. Tuan, J. Phys. B **19**, 1483 (1986).
[16] B. Hird, R. A. Armstrong, and P. Gauthier, Phys. Rev. A **49**, 1107 (1994).
[17] Since the c_i parameters for the Oen and Robinsen straggling loss formalism are unknown for F^+, the corresponding values for Ne^+ [8] were used instead.
[18] NIST Atomic Spectra Database, http://physics.nist.gov/cgi-bin/AtData/levels_form.
[19] Distances are based on the location of maximum radial electron density. Orbital data are taken from J. Slater, *Quantum Theory of Atomic Structure* (McGraw-Hill, New York, 1960), Vol. 1.
[20] R. Morgensten, A. Niehaus, and G. Zimmermann, J. Phys. B **13**, 4811 (1980).
[21] R. Souda, K. Yamamoto, W. Hayami, T. Aizawa, and Y. Ishizawa, Phys. Rev. Lett. **75**, 3552 (1995).
[22] Unrestricted Hartree-Fock calculation at the STO-3G* level using the GAMESS package; W. H. Hehre, R. F. Stewart, and J. A. Pople, J. Chem. Phys. **51**, 2657 (1969); M. W. Schmidt *et al.*, J. Comput. Chem. **14**, 1347 (1993).
[23] For smaller deflection angles, corresponding to ions involved in more glancing collisions, it can be shown that even larger deviations from BCA and, thus, lower exit energies are possible.